Supporting Information

Efficient Liquid Nitrogen Exfoliation of MoS_2 Ultra-Thin Nanosheets in Pure 2H Phase

Honglei Wang,[†,#] Wenzhen Lv,[†,#] Jun Shi,[†] Hongguang Wang,[‡] Dexu Wang,[†] Lu Jin,[†] Jie Chao,[†] Peter A. van Aken,[‡] Runfeng Chen,[†,] Wei Huang[†,$]*

[†] Key Laboratory for Organic Electronics and Information Displays & Jiangsu Key Laboratory for Biosensors, Institute of Advanced Materials (IAM), Jiangsu National Synergetic Innovation Center for Advanced Materials (SICAM), Nanjing University of Posts and Telecommunications (NUPT), Nanjing, 210023, China.

E-mail: iamrfchen@njupt.edu.cn.

[‡] Max Planck Institute for Solid State Research, Heisenbergstrasse 1, 70569, Stuttgart, Germany.

[$] Shaanxi Institute of Flexible Electronics (SIFE), Northwestern Polytechnical University (NPU), Xi'an 710072 China.

This supporting information contains 1 table and 15 figures in 12 pages.

1 Experimental

Chemicals. Molybdenum sulfide (MoS_2) powders (with flake sizes about 2 μm, purity of 99%) was purchased from Sigma-Aldrich. 3,4,9,10-perylenetetracarboxylic acid anhydride (PTCA), N-methyl-2-pyrrolidone (NMP) (99%), isopropanol (IPA) (99%), chloroform (99%), and ethanol (99%) were purchased from Sigma-Aldrich. Other chemicals are of analytical grade and used without further purification. Liquid nitrogen ($L\text{-}N_2$) was purchased from the company of Yehao gas.

Characterization. The morphology of the prepared MoS_2 nanosheets was characterized using a JOEL JEM-1230 transmission electron microscope (TEM) and atom force microscopy (AFM) equipped with a Dimension 3100 (Veeco, CA) in Height mode. High-resolution TEM (HRTEM) characterization was performed on a TECNAI G2 F20 S-Twin delectron microscope. Scanning transmission electron microscopy (STEM) investigations were carried out using a spherical aberration-corrected microscope (JEOL JEM-ARM 200F) with a DCOR probe corrector (CEOS GmbH) at 200 kV. The Raman studies of the films were carried out on a WITec CRM200 confocal Raman microscopy system with a laser excitation energy of 488 nm and an air cooling charge coupled device (CCD) as the detector. The scanning electron microscopy (SEM) images were obtained by Hitachi S-4800. X-ray photoelectron spectroscopy (XPS) data were collected using a PHI 3056 spectrometer with an Al anode source operated at 15 kV and an applied power of 350 W with samples mounted on indium foil. X-ray diffraction (XRD) patterns were obtained using a Rigaku miniflex II. UV-Vis absorption spectra was obtained from a Shimadzu UV-3600 spectrophotometer. The

photograph was taken using a commercial Nikon camera.

2 Table Part

Table S1. Summary of the recently reported nonvolatile WORM memory device performance

Active layer[a]	ON/OFF ratio	Retention time	Reference
PVK	10^4	10^4 s	[1]
BTDBPI	10^4	3.6×10^3 s	[2]
Au NPs:lignin	5×10^3	10^3 s	[3]
PI(TPF-Ph-OMe)	10^5	3.6×10^3 s	[4]
Cu_xO	10^4	10^4 s	[5]
$CsPbBr_3$	10^4	1.2×10^3 s	[6]
AlO_x-native	10^4	10^3 s	[7]
MoS_2-PCBM	10^2	/	[8]
MoS_2-PTCA	10^5	10^4 s	This Work

[a] PVK is Poly(9-vinylcarbazole), BTDBPI is aromatic polyimide, Au NPs:lignin is gold nanoparticles embedded alkali lignin, PI(TPF-Ph-OMe) is poly(4,4'-(2,7-bis(3,5-dimethoxyphenyl)-9H-fluorene-9,9-diyl)dianiline), PCBM is [6,6]-phenyl-C_{61}-butyric acid methyl ester.

3 Figure parts

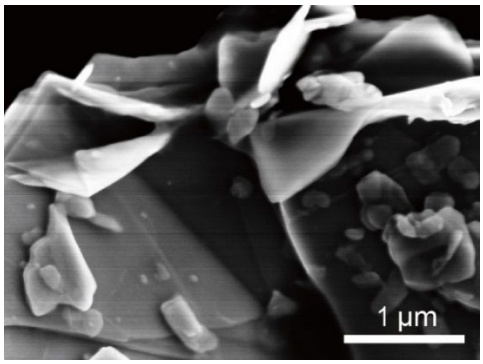

Figure. S1 SEM image of MoS_2-5N acquired after centrifugation at 1500 rpm.

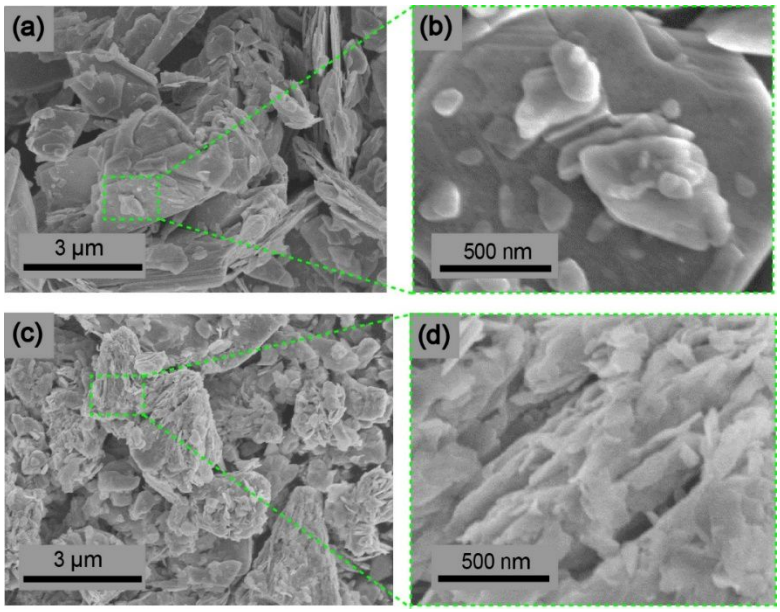

Figure. S2 (a) SEM images and (b) the corresponding enlarged images of bulk MoS_2;

(c) SEM images and (d) the corresponding enlarged images of p-MoS_2-5N.

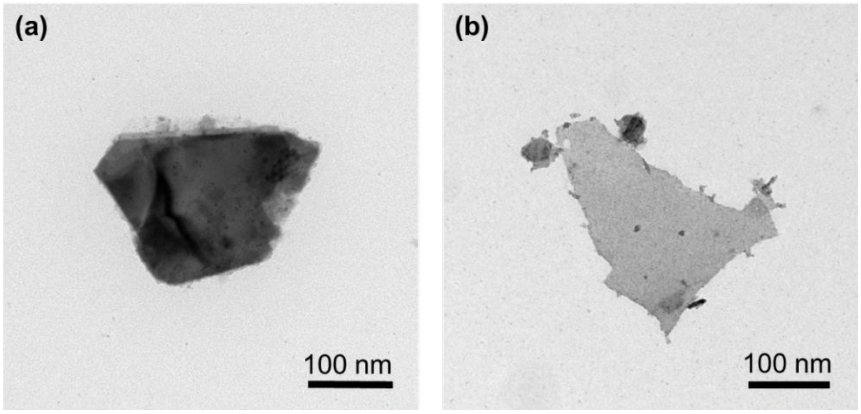

Figure. S3 TEM images of (a) MoS_2-3N and (b) MoS_2-10N.

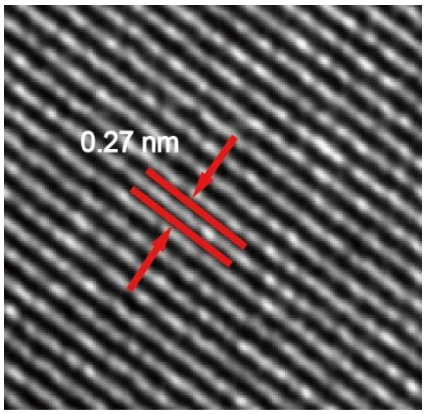

Figure. S4 HRTEM image of MoS_2-5N.

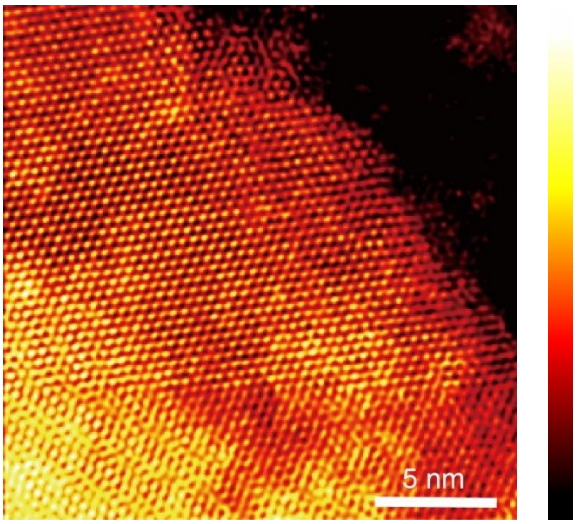

Figure. S5 STEM image of MoS_2-5N. From dark to yellow, the layer thickness of MoS_2 increases.

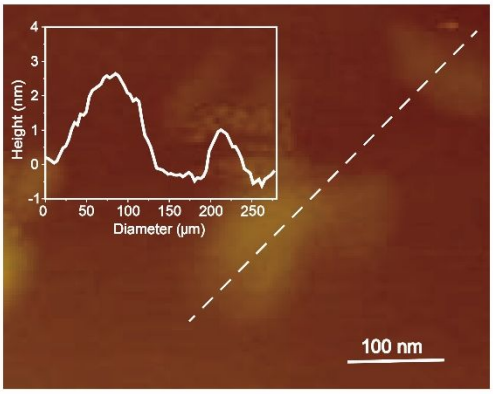

Figure. S6 AFM image and height profile (inset) of MoS_2-5N.

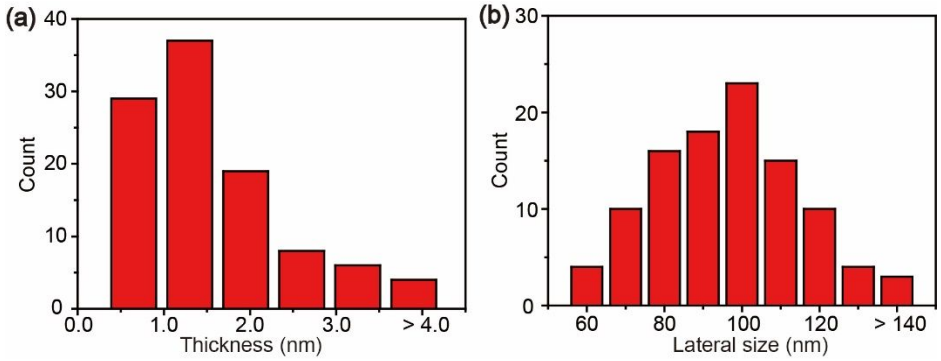

Figure. S7 Thickness (a) and lateral size (b) distributions of MoS_2-5N.

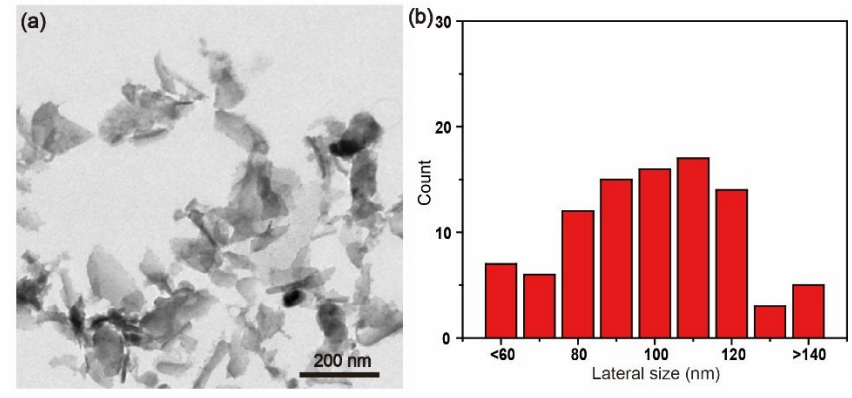

Figure. S8 TEM image (a) and corresponding lateral size distribution (b) of MoS_2-5N.

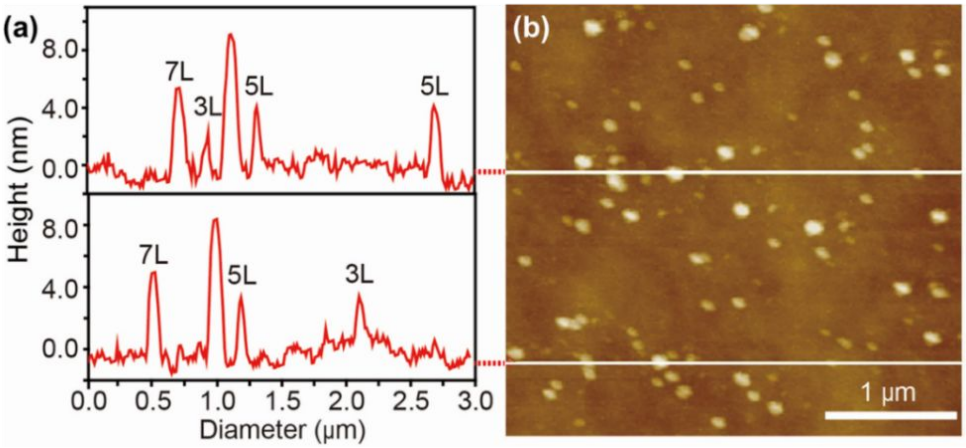

Figure. S9 AFM height profiles (a) and image (b) of MoS_2-3N.

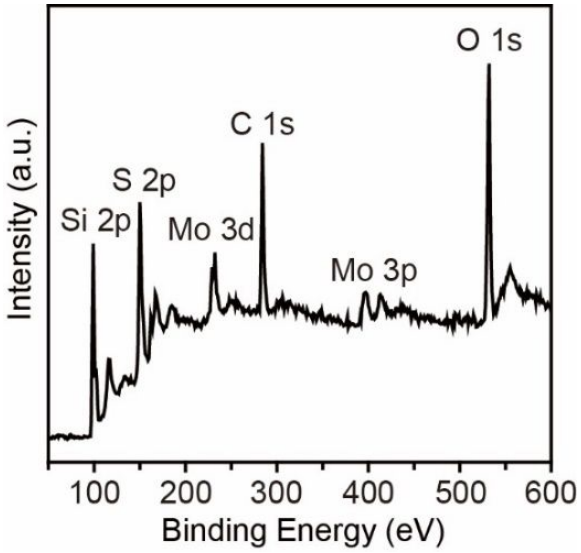

Figure. S10 XPS survey spectrum of MoS_2-5N.

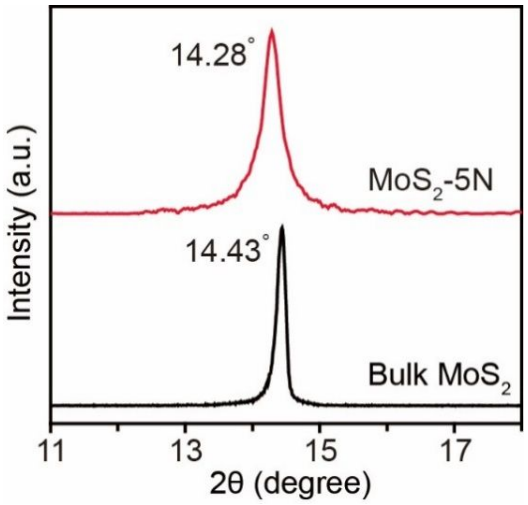

Figure. S11 Enlarged XRD patterns of bulk MoS_2 and MoS_2 -5N.

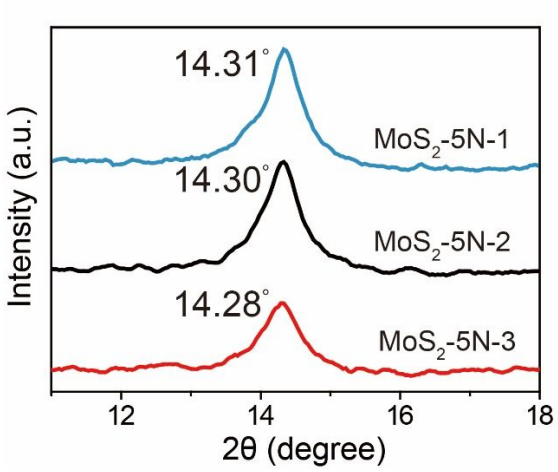

Figure. S12 Enlarged XRD patterns of different MoS_2 -5N.

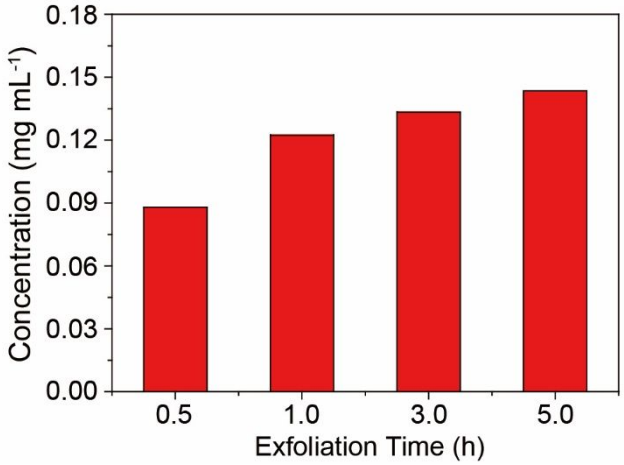

Figure. S13 Concentration versus exfoliation time of the liquid nitrogen exfoliation of MoS_2.

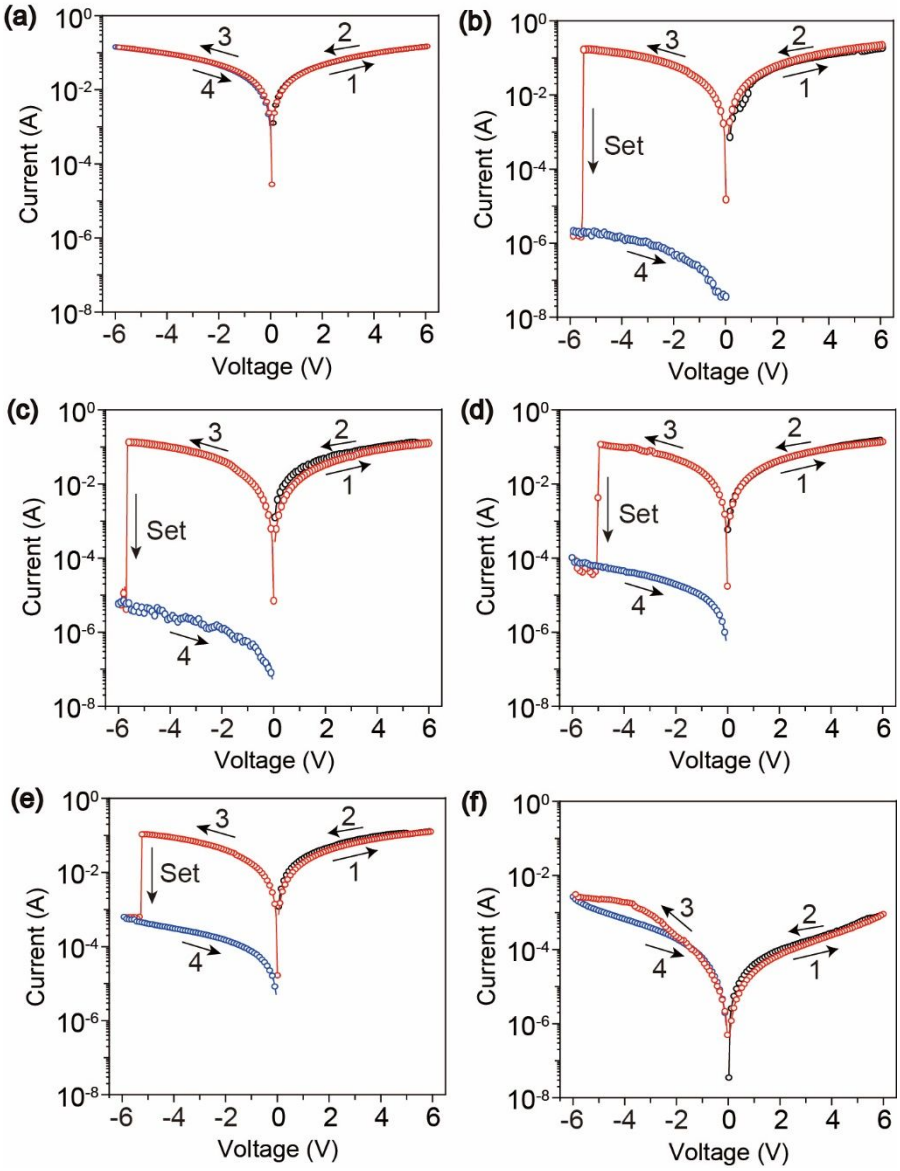

Figure. S14 I−V characteristics of the ITO/ PTCA (x wt %)-MoS_2/Al diode memory devices, where x = 0, 5, 15, 30, 50 and 100 for panels of (a), (b), (c), (d), (e) and (f), respectively.

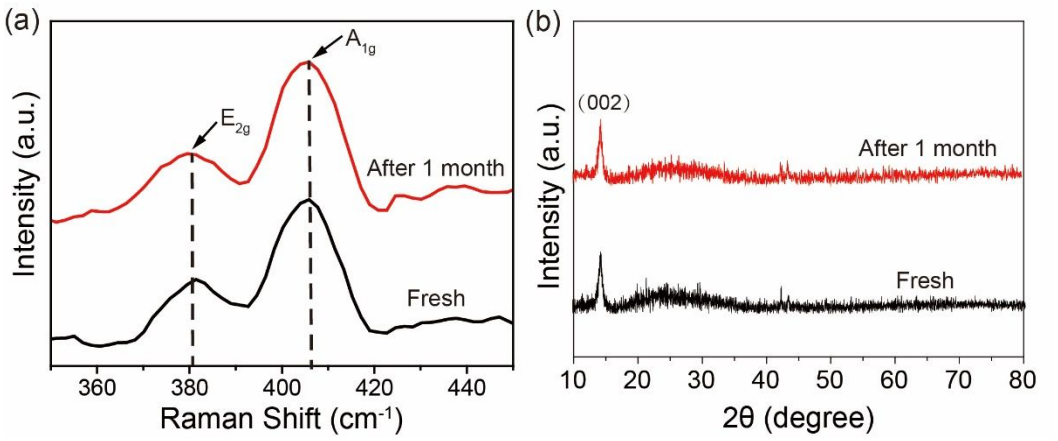

Figure. S15 Raman spectra (a) and XRD patterns (b) of the freshly prepared PTCA (5 wt %)-2H MoS_2 composite and that after store at room temperature for 1 month.

REFERENCE

[1] Ban, C.; Wang, X.; Zhou, Z.; Mao, H.; Cheng, S.; Zhang, Z.; Liu, Z.; Li, H., Liu, J.; Huang, W. A Universal Strategy for Stretchable Polymer Nonvolatile Memory via Tailoring Nanostructured Surfaces. *Sci. Rep.* **2019**, *9*, 10337, DOI 10.1038/s41598-019-46884-4.

[2] Qu, L.; Tang, L.; Bei, R.; Zhao, J.; Chi, Z.; Liu, S.; Chen, X.; Aldred, M. P.; Zhang, Y.; Xu, J. Flexible Multifunctional Aromatic Polyimide Film: Highly Efficient Photoluminescence, Resistive Switching Characteristic, and Electroluminescence. *ACS Appl. Mater. Inter.* **2018**, *10* (14), 11430-11435, DOI 10.1021/acsami.8b02712.

[3] Wu, W.; Han, S.-T.; Venkatesh, S.; Sun, Q.; Peng, H.; Zhou, Y.; Yeung, C.; Li, R. K. Y.; Roy, V. A. L. Biodegradable Skin-Inspired Nonvolatile Resistive Switching Memory Based on Gold Nanoparticles Embedded Alkali Lignin. *Org. Electron.* **2018**, *59*, 382-388, DOI 10.1016/j.orgel.2018.05.051.

[4] Yang, Y.; Xia, J.; Ding, Z.; Zheng, Y.; Ding, S.; Shen, Y. Synthesis and Resistive Switching Characteristics of Polyimides Derived from 2,7-Aryl Substituents Tetraphenyl Fluorene Diamines. *Eur. Polym. J.* **2018**, 108, 85-97, DOI 10.1016/j.eurpolymj.2018.08.040.

[5] Hsu, C.-C.; Tsai, J.-E.; Lin, Y.-S. A Write-Once-Read-Many-Times Memory Based

on A Sol-Gel Derived Copper Oxide Semiconductor. *Physica B* **2019**, 562, 20-25, DOI 10.1016/j.physb.2019.03.007.

[6] Chen, Z.; Zhang, Y.; Yu, Y.; Che, Y.; Jin, L.; Li, Y.; Li, Q.; Li, T.; Dai, H.; Yao, J. Write Once Read Many Times Resistance Switching Memory Based on All-Inorganic Perovskite $CsPbBr_3$ Quantum Dot. *Opt. Mater.* **2019**, 90, 123-126, DOI 10.1016/j.optmat.2019.01.069.

[7] Avila-Nino, J. A.; Reyes-Reyes, M.; Nunez-Olvera, O.; Lopez-Sandoval, R. A Simple Method for Fabrication of Antifuse WORM Memories. *Appl. Surf. Sci.* **2018**, 454, 256-261, DOI 10.1016/j.apsusc.2018.05.126.

[8] Lv, W.; Wang, H.; Jia, L.; Tang, X.; Lin, C.; Yuwen, L.; Wang, L.; Huang, W.; Chen, R. Tunable Nonvolatile Memory Behaviors of PCBM–MoS_2 2D Nanocomposites through Surface Deposition Ratio Control. *ACS Appl. Mater. Inter.* **2018**, *10* (7), 6552-6559, DOI 10.1021/acsami.7b16878.